Arabian Journal of Chemistry (2023) **16**, 104954

King Saud University

Arabian Journal of Chemistry

www.ksu.edu.sa
www.sciencedirect.com

ORIGINAL ARTICLE

Selection of bioactive chemical markers for anti-aging skin assessment of *Dimocarpus longan* Lour. leaf extract

Pimjai Doungsaard [a], Sunee Chansakaow [b], Worrapan Poomanee [b,c], Busaban Sirithunyalug [b], Siripat Chaichit [d], Pimporn Leelapornpisid [b,c,*]

[a] *Faculty of Pharmacy, Chiang Mai University, Chiang Mai 50200, Thailand*
[b] *Department of Pharmaceutical Sciences, Faculty of Pharmacy, Chiang Mai University, Chiang Mai 50200, Thailand*
[c] *Innovation Center for Holistic Health, Nutraceuticals and Cosmeceuticals, Faculty of Pharmacy, Chiang Mai University, Chiang Mai 50200, Thailand*
[d] *Laboratory for Molecular Design and Simulation (LMDS), Faculty of Pharmacy, Chiang Mai University, Chiang Mai 50200, Thailand*

Received 16 January 2023; accepted 25 April 2023
Available online 2 May 2023

KEYWORDS

Dimocarpus longan;
Bioactive chemical markers;
Anti-aging;
Phytochemistry;
Molecular docking;
HPLC fingerprint

Abstract Hydroethanolic longan (*Dimocarpus longan Lour.*) leaf extract has reported remarkable biological activities related to the aging process for use in cosmeceuticals. Finding the bioactive chemical marker (BCM) could play a crucial role for cosmeceutical manufacturers in guaranteeing the quality of the extract and its efficacy. This study aimed to select the most potential BCM established and predicted for the anti-aging skin of hydroethanolic longan leaf extract. The assessment of anti-aging of the skin was determined by evaluating *in vitro* antioxidant activities, including 2,2-diphenyl-1-picrylhydrazyl (DPPH) radical scavenging and inhibiting lipid peroxidation assay. Furthermore, anti-hyaluronidase and anti-collagenase activity were also determined. The extract underwent bioassay-guided fractionation using normal phase preparative-thin layer chromatography. Ethyl gallate in the fractionated extract possessed biological activities as a high proportion part. The strong positive linear relationship between DPPH scavenging, lipid peroxidation inhibition, anti-collagenase, and anti-hyaluronidase activity ($r = 0.997$, 0.972, 0.998, and 0.998, respectively) under the deterioration of the ethyl gallate was shown. The molecular docking of ethyl gallate to collagenase and hyaluronidase resulted in a good and acceptable binding affinity. Therefore, ethyl gallate could be potentially used as a bioactive chemical marker for hydroethanolic longan leaf

* Corresponding author at: Suthep Road, Suthep, Muang, Chiang Mai 50200, Thailand.
E-mail address: pimporn.lee@cmu.ac.th (P. Leelapornpisid).
Peer review under responsibility of King Saud University. Production and hosting by Elsevier.

Production and hosting by Elsevier

https://doi.org/10.1016/j.arabjc.2023.104954

extract in pharmaceutical and cosmeceutical applications.

1. Introduction

Aging is characterized by an organism's progressive functional decline, leading to increased susceptibility to age-related diseases, including cardiovascular disease, neurogenerative disease and skin aging. Skin is the largest and most important organ that serves as a protective barrier against the external environment and harmful agents. Skin aging is a complex process determined by intrinsic and extrinsic factors, leading to a progressive loss of structural integrity and physiological function (Naidoo and Birch-Machin, 2017). Dermatologic disorders such as wrinkling, scaling and dryness could develop into various skin diseases. Moreover, an abnormal skin appearance leads to a lack of self-confidence and a decreased quality of life. (Nichols and Katiyar, 2010). Oxidative stress is a major player in both extrinsic and intrinsic skin aging processes (Rinnerthaler et al., 2015). The excessive and uncontrolled generation of reactive oxygen species (ROS) is the main cause of oxidative stress. ROS could directly cause cellular damage cellular and stimulate matrix metalloproteinases (MMPs), including collagenase and hyaluronidase. Consequently, extracellular matrix (ECM) and protein filament breakdown occur (Kolarsick et al., 2011; Kurtz and Oh, 2012; Sharadha et al., 2020). Collagen, a major structural fibrous protein of the extracellular matrix (ECM) in the skin, is degraded by a group of MMPs known as collagenase. The degradation of collagen leads to the disorganization of skin structure, causing skin wrinkles (Pittayapruek et al., 2016). Hyaluronic acid, the largest extracellular matrix, retains the skin's hydration, structure, and elasticity. The activation of hyaluronidase mainly induces the gradation of hyaluronic acid, reducing skin moisture and tension. (Manuskiatti et al., 1996). Thus, antioxidants, collagenase and hyaluronidase activity inhibitors could sustain skin elasticity by delaying ROS generation, and skin collagen and hyaluronic acid degradation can be used for anti-aging assessment.

Longan (*Dimocarpus longan* Lour.) is a well-known tree species of the Sapindaceae family, widely distributed in subtropical zones such as Southeastern Asian countries and Southern China for commercial purposes (Paul et al., 2021). The longan industry produces many byproducts, such as leaves trimmed to increase fruit productivity. The longan leaf extracts contain various phytochemicals, including phenolics, flavonoids, terpenoids and sterols (Xue et al., 2015; Liu et al., 2012). Several studies investigated their antioxidant potential. According to Ripa et al. (2010), the methanol extract of longan leaves was semi-purified using liquid–liquid extraction with petroleum ether, chloroform and ethyl acetate. The extracts showed the ability to scavenge 2,2-diphenyl-1-picrylhydrazyl (DPPH) radicals at the same level of ascorbic acid, with the IC_{50} value of ascorbic acid, petroleum ether extract, chloroform extract and ethyl acetate extract of 43.11, 50.95, 44.28 and 44.31 μg/ml, respectively. In the study of Chen et al. (2017), the extract of longan leaves obtained from 40% ethanolic extraction exhibited the ability to scavenge DPPH and ABTS radicals equivalent to Trolox at 218.67 and 582.37 μmol, respectively. Moreover, the extract showed ferric-reducing antioxidant power (FRAP) equivalent to 182.58 μmol of Trolox. Additionally, our previous study declared that the anti-aging potentials of hydroethanolic longan leaf extract could inhibit hyaluronidase and collagenase activities with IC_{50} of 234.80 ± 21.52 and 314.44 ± 62.14 μg/ml, respectively (Doungsaard et al., 2020). According to biological activities, hydroethanolic longan leaf extract could be a valuable ingredient for anti-aging in the cosmeceutical industry. However, there is insufficient data in chemical marker-based standardization of hydroethanolic longan leaf extract.

The overall quality of botanical extract was affected by many factors, including the extraction procedure, seasonal changes, harvesting time, cultivation sites, post-harvesting processing, adulterants, and raw materials substitutes. As a consequence of economic factors, it would only be applicable to determine some of the constituents in the botanical extract. Chemical markers-based standardization plays a crucial role for manufacturers in the quality control of herbal products (Yang et al., 2017). The present study aims to firstly establish and select a bioactive chemical marker (BCM) for anti-aging assessment, which could predict the pharmacologic bioactivity of hydroethanolic longan leaf extract. The achievement of this study potentially renders a bioactive chemical marker for hydroethanolic longan leaf extract in pharmaceutical and cosmeceutical applications, including quality control and product development. The bioactive compounds were identified using bioassay-guided isolation. A conventional chromatographic technique, preparative thin-layer chromatography, was employed. The collected fractions were continuously screened for the skin's anti-aging ability, summarized as *in vitro* DPPH radical scavenging, inhibition of lipid peroxidation, anti-collagenase, and anti-hyaluronidase activity. Then the BCM was uncovered using the Adjusted Efficacy Score (AES)-based method and verified by the correlation between the BCM amount and the activities of the extract after one month of accelerated storage.

2. Material and methods

2.1. Chemical material

2,2′-Azobis(2-amidinopropane) dihydrochloride (AAPH) and linoleic acid were purchased from Fluka (Buchs, Switzerland). Acetonitrile, ammonium thiocyanate, boric acid, calcium chloride, iron (II) chloride tetrahydrate, sodium borate, and sodium metaborate were purchased from Merck (Darmstadt, Germany). 2,2-diphenyl-1-picrylhydrazyl (DPPH),3,4-dihydroxyphenaylacetic acid (3,4-DHPAA), 4-dimethylaminobenzaldehyde (DMAB), bovine collagen, collagenase type 1A from *Clostridium histolyticum*, ellagic acid, Folin-Ciocalteu reagent, gallic acid, hyaluronic acid sodium salt from *Streptococcus equi*, hyaluronidase from bovine testes and sodium periodate were purchased from Sigma-Aldrich (St. Louis, MO, USA). Ethyl gallate was purchased from Tokyo Chemical Industry (Tokyo, Japan). Ethanol (95%) for extraction was purchased from Liquor Distillery Organization (Chachoengsao, Thailand), and deionized water, used for extraction, was generated by Millipore Milli-Q Advantage (Merck).

2.2. Collection of plant materials and extract preparation

D. longan cv. E-Daw mature leaves were collected from a longan farm in Chiang Mai Province, Thailand, from April to May 2019. After washing through with tap water, they were dried at 50 °C for 24 h and ground to powder. After passing through an 80-mesh sieve, the powder was subjected to three rounds of maceration in 50%(v/v) aqueous ethanol for 48 h at room temperature and filtered with Whatman filter paper. The filtered extracts were pooled and then dried using a rotary

evaporator (R-300 Buchi®, Flawil, Switzerland) under a pressure of 50 mbar at 50 °C. The hydroethanolic longan leaf extract was collected and stored at −20 °C until further use.

2.3. Fractionation and evaluation of bioactive fractions

. The hydroethanolic longan leaf extract underwent bioassay-guided fractionation via normal phase preparative-Thin Layer Chromatography (Analtech 60F, 1 mm 20x20 cm). The extract (100 mg) was dissolved with 50% (v/v) methanol, then applied on silica prep-TLC as long streaks and developed with ethyl acetate: formic acid: acetic acid: water 100:11:11:26 (v/v/v/v). Zones on the TLC plate were detected under UV light (254 and 366 nm). The visualized bands were scrapped separately in nine fractions. Then each scratch silica gel was eluted with 50% ethanol and filtered to collect the filtrate. All filtrates were dried using a rotary evaporator (R-300 Buchi®, Flawil, Switzerland) under the pressure of 50 mbar at 50 °C and stored at −20 °C. The bioactive chemical marker selection was based on *in vitro* investigation in four aspects of skin anti-aging assessment, including DPPH radical scavenging, inhibiting lipid peroxidation, anti-collagenase, and anti-hyaluronidase activity. Then, the compounds presented in the fractions with the highest Adjusted Efficacy Scores (AES) were further identified by spectroscopic techniques, basically using LC-MS/MS.

2.4. Antioxidant properties

2.4.1. DPPH radical scavenging

DPPH radical scavenging assay was determined according to the method described by Kamma et al. (2019). Hydroethanolic longan leaf extract, all fractionated extracts and standards were dissolved in 50% (v/v) ethanol at 1 mg/ml concentration. The reaction mixture, containing 20 µl of fractionated extract and 180 µl of 200 mM DPPH ethanolic solution, was incubated at room temperature in the dark for 30 min. The absorbance of the mixed solution was measured at 517 nm wavelength using a spectrophotometer (Spectramax M3, San Jose, CA, USA). Gallic acid, ethyl gallate, ellagic acid and astragalin were used as the positive control. Three independent experiments in triplicate were performed in the experiment. The DPPH radical scavenging was calculated using the following formula.

$$\text{DPPH scavenging effect}\,(\%) = \frac{\text{Abs}_{\text{control}} - \text{Abs}_{\text{sample}}}{\text{Abs}_{\text{control}}} x100$$

where $\text{Abs}_{\text{control}}$ was the absorbance value of the reaction mixture when the sample solution was replaced with 50% (v/v) ethanol, and $\text{Abs}_{\text{sample}}$ is the absorbance value of the reaction mixture of the sample solution.

2.4.2. Lipid peroxidation inhibition

The inhibition of lipid peroxidation of hydroethanolic longan leaf extract and each fractionated extract was determined using the ferric thiocyanate (FTC) method following Kamma et al. (2019). All the samples and standards were dissolved in 50% (v/v) ethanol at 1 mg/ml concentration. Then 100 µl aliquot of the sample was added to the mixture containing 140 µl of 1.3% (v/v) linoleic acid in methanol and 140 µl of 20 mM phosphate buffer pH 7.0. Afterward, 20 µl of AAPH (46.35 mM), the lipid peroxidation initiator, was added to start the reaction in the Eppendorf® tube. The reaction mixtures were incubated at 45 °C in the dark for 4 h. The degree of lipid peroxidation was determined using the FTC method when 2.5 µl of the reaction mixture was combined with 2.5 µl of 20 mM $FeCl_2$ solution in 3.5% (v/v) HCl, 2.5 µl of 10% (w/v) NH_4SCN solution and 192.5 µl of 75% (v/v) methanol in a 96-well microplate. After 3 min, the degree of oxidation was measured at 500 nm wavelength using a spectrophotometer (Spectramax M3, San Jose, CS, USA). Gallic acid, ethyl gallate, ellagic acid and astragalin were used as the positive control. Three independent experiments in triplicate were performed in the experiment. The peroxidation inhibition ability was calculated following the DPPH radical scavenging assay method.

2.5. Anti-collagenase activity

The anti-collagenase activity was determined using the method of Yasmin et al. (2014) with some modifications. Hydroethanolic longan leaf extract, all fractionated extracts and standards were dissolved in 20% (w/w) Tween 20® at 1 mg/ml concentration. The mixture containing 30 µl of the sample, 100 µl of 10 mM $CaCl_2$ in 125 mM borate buffer pH 7.5 and 50 µl of 0.1 mg/ml collagenase in 125 mM borate buffer pH 7.5 were incubated in an Eppendorf® tube in the dark at 37 °C for 10 min. After that, the 20 µl of collagen solution (80 µg/ml) was added and then incubated at 37^{O}C for 60 min. The fractionated collagen was detected by fluorescence reaction of the N-terminal side of the glycine with 3,4-DHPAA. Then 200 µl of the enzymatic solution was added to each 200 µl of 0.75 mM DHPAA, 125 mM sodium borate pH 8 and 1.25 mM $NaIO_4$ and then incubated at 37 °C for 10 min, and the fluorophore was stabilized in an ice water bath. Fluorescent intensity was measured using a multi-mode microplate reader (Spectramax M3®, San Jose, CA, USA) at an excitation of 375 nm and an emission of 465 nm wavelength. Gallic acid, ethyl gallate, ellagic acid and astragalin were used as the positive control. Three independent experiments in triplicate were performed in the experiment, and the anti-collagenase activity was calculated using the following formula.

$$\text{Inhibition of collagenase activity} = \frac{(\text{F.I}_{\text{control}}) - (\text{F.I}_{\text{sample}})}{(\text{F.I}_{\text{control}})} \text{x}\,100$$

where F. $\text{I}_{\text{control}}$ was the fluorescent intensity of the reaction mixture when the sample solution was replaced with 20% (w/w) Tween20® and F. $\text{I}_{\text{control}}$ is the fluorescent intensity of the reaction mixture of sample solution.

2.6. Anti-hyaluronidase activity

The anti-hyaluronidase activity was determined using the fluorometric Morgan-Elson assay modified by Takahashi et al. (2003) with some modifications. Hydroethanolic longan leaf extract, all fractionated extracts and standards were dissolved in 20% (w/w) Tween 20® at 1 mg/ml concentration. Briefly, the mixture containing 12.5 µl of extract, 25 µl of 12.5 mM calcium chloride and 12.5 µl of 1.5 mg/ml was incubated in an Eppendorf® tube in the dark at 37 °C for 20 min. Then

100 µl of hyaluronic acid (1 mg/ml) in 0.1 M acetate buffer pH 3.5 was added and incubated for 60 min at 37 °C. Afterward, the mixture was alkalized by 25 µl of 0.8 M sodium metaborate and then boiled to 100 °C for 3 min to complete the Morgan-Elson reaction. After cooling to room temperature, 50 µl of the reaction mixture was transferred to each well of the 96-well microplate. The 150 µl of DMAB reagent containing 4 g of DMAB in 40 ml of acetic acid and 5 ml of 10 N HCl was added to each well and incubated for 20 min before measuring the fluorophore by a multi-mode microplate reader (Spectramax M3®, San Jose, CA, USA) at an excitation of 545 nm and an emission of 612 nm. Gallic acid, ethyl gallate, ellagic acid and astragalin were used as the positive control. Three independent experiments in triplicate were performed in the experiment. The inhibition of anti-hyaluronidase activity was calculated using the same equation as anti-collagenase activity.

2.7. Establishment of bioactive chemical markers identified based on Adjusted efficacy score (AES)

As the content of the bioactive compounds was also an important factor in representing the importance of the constituent in botanical extract, the AES was applied to identify BCM of longan leaf hydroethanolic extract. The equation for the AES calculation was presented as follows.

$$AES(a) = \frac{c(a)x\,ES\,(a)}{\sum_{a=1}^{w}\{c(a)xES(a)]}x100$$

where $c(a)$ is the content of constituent a, ES (a) is the efficacy score which is % inhibition of each activity, and w is the number of constituents quantified (Yang et al., 2017).

2.8. LC-MS/MS analysis

Phytochemical analysis of bioactive compounds was performed using a Liquid Chromatography-Mass Spectrometry system (LC-MS). Specifically, the system consisted of an LC-MS Agilent 6500 Series Accurate-Mass Quadrupole Time-of-Flight Detector (Q-TOF-MS) (Agilent Technologies, Inc., Santa Clara, CA, USA) with ESI-Jet Stream as the electrospray ionization method. Zorbax Eclipse Plus C18 (2.1 × 50 m m, 1.8 µm) was purchased from Merck (Darmstadt, Germany). The mobile phases were A: H_2O 0.1% formic acid and B: acetonitrile 95% 0.1% formic acid. The elution gradient was applied at a flow rate of 0.50 ml/min, while the total duration of analysis was 22 min. The following gradient (A: B) was used: 0 min (98:2), 15 min (0:100), 20 min (98:2) and 22 min (98:2). The injection volume of the sample was 10 µl. Mass spectrometry samples were ionized by the negative ion mode of ESI (Electro Spray Ionization). Data were analyzed using Agilent MassHunter Software (Version B.06.00, Agilent Technologies, USA). Phenolic constituents were identified by comparing their mass spectra and fragmentation patterns with the literature data.

2.9. Correlations between the bioactive compounds and the biological activities

Hydroethanolic longan leaf extract solution was prepared by diluting the extract with 20% (w/w) Tween 20® in deionized water at 2 mg/ml concentration. The solution was kept in amber glass bottles and stored under 4, 25, and 45 ± 0.5 °C for one month. The storage was performed to deteriorate the amount of each bioactive compound which was crucial in reducing anti-aging activity. After storage, the HPLC analysis for bioactive compounds and *in vitro* investigation in four aspects of anti-aging skin assessment was evaluated. The correlation between the area under chromatographic peaks of bioactive compounds and biological activities after one month storage was calculated to verify the predictability of BCM.

2.10. High-Performance liquid Chromatography (HPLC) - ultraviolet (UV) detection analysis

The hydroethanolic longan leaf extract and fractionated extract were also analyzed by HPLC-UV analysis employing the system of the previous study (Doungsaard et al., 2020). Briefly, HPLC analysis was performed by a C-18 column (250x4.6 mm, ODS-3, i.d., 5 µm, Inertsil^{TM}, GL Sciences, Japan) as a stationary phase. The mobile phases were A: acetonitrile and B: 0.1% phosphoric acid. The elution gradient was applied at a flow rate of 0.90 ml/min at room temperature, while the total duration of analysis was 50 min. The following gradient (A: B) was used: 0 min (10:90), 50 min (30:70). The standard and extract were filtered through 0.22 µm nylon syringe filters (ALWSCI Corporation, China). The 10 µl of standard and sample was injected in the HPLC column and detected at 280 nm.

2.11. Molecular docking simulation

Molecular docking was used to investigate the binding interactions of ethyl gallate, gallic acid, and ellagic acid towards collagenase and hyaluronidase. The possible binding mode of ethyl gallate, gallic acid, and ellagic acid towards collagenase and hyaluronidase was modeled using molecular docking. In this study, AutoDock Vina 1.1.2 was used to perform the molecular docking simulation (Trott and Olson, 2010). The three-dimensional structures of each compound were retrieved from the PubChem database (https://pubchem.ncbi.nlm.nih.gov/). All ligand structures underwent optimized calculation using Gaussian09 with the PM6 semi-empirical method (Stewart, 2009). Subsequently, hydrogen atoms and Gasteiger's charges were assigned using AutoDockTools 1.5.6 (Morris et al., 2009). The human crystal structures of collagenase (PDB ID: 1CGL) (Lovejoy et al., 1994) and hyaluronidase (PDB ID: 2PE4) (Chao et al., 2007) were obtained from the Protein Data Bank (PDB) database (https://www.rcsb.org/). The water molecules and co-crystallized ligands were removed from the structures. A grid center for collagenase was set at X: 30.681, Y: 46.555, and Z: −0.0090, while that of hyaluronidase was centered at X: 41.945, Y: −21.787, and Z: −16.336. After performing the docking simulation, the conformer with the lowest binding score (kcal/mol) was selected for analysis. Molecular recognition was defined using LigandScout 4.4.8 (Wolber and Langer, 2005), and the binding modes of promising compounds were visualized in the PyMOL2 software (Schrodinger, 2015).

2.12. Statistical analysis

All experiments in this study were conducted in triplicate. The results were expressed as the mean ± standard deviation and analyzed using the SPSS Version 25.0 Program. One-way analysis of variance (ANOVA) with Tukey's test was carried out to test significant differences at the probability level of 0.05. Pearson correlations between variables were established using the SPSS Version 25.0 Program.

3. Results and discussion

3.1. Fractionation of hydroethanolic longan leaf extract

Thin Layer Chromatography was performed using ethyl acetate: formic acid: acetic acid: water 100:11:11:26 (v/v/v/v). This solvent system is suitable for investigating phenolic compounds as the related study concluded that the activities of the extract might be involved in phenolic compounds (Medić-Šarić et al., 1996; Doungsaard et al., 2020). The extract was fractionated in nine portions according to TLC Chromatogram, as shown in Fig. 1. Under UV-254 nm, the extract showed the four prominent fluorescence-quenching zones in the Rf range 0.9 to 0.7, which were defined as fractions 1, 2, 4 and 5. Under UV-365 nm, the red fluorescence was indicated as chlorophyll, while the blue-fluorescence zones at Rf ~ 0.8 and 0.4 were defined as fractions 4 and 7. The unclear zone upper and under fraction 7 were defined as fractions 6 and 8. The zone left on the start point was defined as fraction 9.

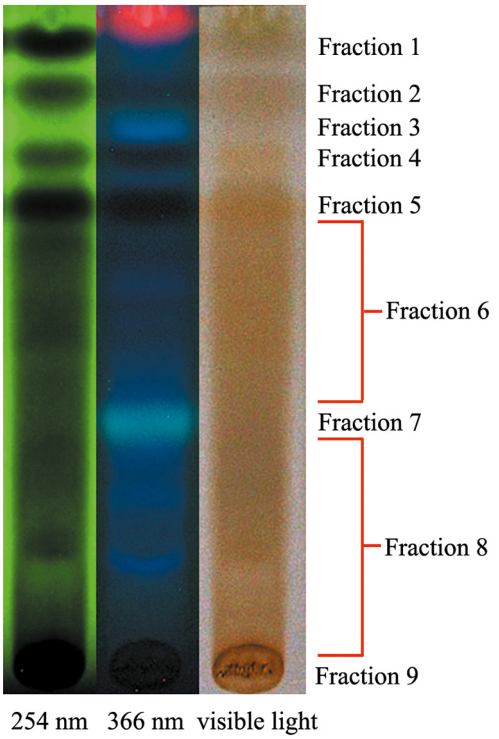

Fig. 1 TLC Chromatogram of hydroethanolic longan leaf extract under the UV-254, 366 nm and white light using ethyl acetate: formic acid: acetic acid: water 100:11:11:26 (v/v/v/v) as a mobile phase. The extract was fractionated into nine portions.

The % yields of each fraction are presented in Table 1. The high yields were presented at fractions 1,6, 7 and 8. This TLC system's lower polarity compounds or aglycone usually migrated to the solvent front. In contrast, the polar compounds or glycosides were presented at low Rf values (Wagner and Bladt, 1996), indicating that most constituents were polar compounds.

3.2. Antioxidant properties

The antioxidant activities, including DPPH scavenging and inhibiting lipid peroxidation of hydroethanolic longan leaf extract, all fractionated extracts, and standards, are presented in Table 1. DPPH radical is characterized as a stable free radical by delocalizing the spare electron all over the molecule. The electron delocalization gives a violet color, absorbing the wavelength at about 517 nm. When the antioxidant donates to the hydrogen atom, the rise of the DPPH-reduced form occurs with the loss of violet color (Alam et al., 2013). The DPPH radical scavenging assay was a simple test system that first indicates radical scavenging potential. Hence, this method is accurate, easy to perform and suitable for industrial applications (Gerhäuser, 2009). The results showed that all the fractions possessed different levels of DPPH scavenging activity at the reaction concentration of 100 µg/ml. Fractions 1 and 2 showed the highest activity at 83.05 ± 5.45 and 79.66 ± 8.79 % of inhibition, respectively.

Lipid peroxidation is an oxidation process when polyunsaturated fatty acid is in the human body, especially on the cell membrane. The result is the breakdown of the cell membrane and the generation of reactive aldehydes, which can induce the damage of cellular constituents and activate signaling pathways initiating cell death. Consequently, skin cells damage and tissue structural diminishment manifested as the formation of wrinkles and aging (Juan et al., 2021). In hydroethanolic longan leaf extract, all fractionated extracts and standards presented the homogenous level of inhibiting lipid peroxidation, about 30–60%, at the reaction concentration of 250 µg/ml.

Since ROS is closely related to skin aging, using antioxidants may serve as a promising strategy for slowing aging. The present study found that the crude hydroethanolic longan leaf extract and fractionated extracts, especially fractions 1 and 2, are potent antioxidants comparable to standards. However, the crude extract is more suitable than the purified extract in industrial applications from an economic viewpoint.

3.3. Anti-collagenase activity

Collagen is a major structural fibrous protein of the extracellular matrix (ECM) in the skin. Collagenase is an enzyme involved in collagen hydrolysis and plays an important role in collagen degradation, leading to the disorganization of skin structure and causing skin wrinkles. (Pittayapruek et al, 2016). The anti-collagenase activity of hydroethanolic longan leaf extract, all fractions and standards were measured at the reaction concentration of 150 µg/ml. As detailed in Table 1, fractions 4,6 and 7 could not inhibit collagenase enzyme. In contrast, hydroethanolic longan leaf extract, fractions 1 and 2, had a strongly anti-collagenase activity comparable to gallic acid and ethyl gallate. Thus, fractions 1, 2 and hydroethanolic

Table 1 Yields and biological activities of the hydroethanolic longan leaf extract, its fractionated extracts, and standards.

Sample	%Yield	% Inhibition			
		DPPH scavenging assay	Lipid peroxidation inhibitory activity	Anti-collagenase activity	Anti-hyaluronidase activity
Hydroethanolic longan leaf extract	16.12 ± 1.87^{a}	81.85 ± 5.24^{a,b}	49.89 ± 1.30^{a,b}	43.90 ± 14.32^{a}	52.62 ± 14.23^{a,b,c,d}
Fr. 1	7.90 ± 2.54^{b}	83.05 ± 5.45^{a,b}	52.85 ± 6.56^{a,b}	45.19 ± 6.45^{a}	67.96 ± 8.16^{a}
Fr. 2	2.61 ± 0.27^{d}	79.66 ± 8.79^{a}	55.20 ± 5.75^{a,b}	37.28 ± 8.55^{b}	63.82 ± 5.52^{a,b,c,d}
Fr. 3	3.82 ± 0.43^{c,d}	18.15 ± 6.41^{c,d}	38.13 ± 7.46^{a}	13.75 ± 8.17^{b}	34.05 ± 4.14^{c,d}
Fr. 4	2.80 ± 0.92^{d}	22.83 ± 4.52^{c,d,e}	40.88 ± 15.55^{a,b}	ND	36.31 ± 7.15^{b,c,d}
Fr. 5	5.79 ± 0.33^{b,c,d}	27.02 ± 6.75^{d,e,f}	56.17 ± 8.32^{a,b}	11.46 ± 4.48^{b}	34.51 ± 7.20^{c,d}
Fr. 6	8.44 ± 1.90^{b}	38.51 ± 6.46^{e,f}	42.11 ± 9.56^{a,b}	ND	30.67 ± 11.58^{d}
Fr. 7	9.19 ± 1.34^{b}	13.10 ± 2.55^{c,d}	50.10 ± 4.52^{a,b}	ND	39.31 ± 6.54^{a,b,c,d}
Fr. 8	8.63 ± 1.94^{b}	8.15 ± 4.64^{c}	42.06 ± 5.54^{a,b}	17.73 ± 7.46^{b}	40.34 ± 4.12^{a,b,c,d}
Fr. 9	6.58 ± 0.84^{b,c}	19.44 ± 9.21^{c,d}	43.25 ± 8.65^{a,b}	14.27 ± 5.43^{b}	37.82 ± 7.54^{b,c,d}
Standards					
Gallic acid	–	92.35 ± 0.50^{b}	49.97 ± 5.16^{a,b}	46.35 ± 1.48^{a}	64.39 ± 15.38^{a,b}
Ethyl gallate	–	87.65 ± 0.88^{b}	60.23 ± 2.23^{b}	42.25 ± 3.02^{a}	62.35 ± 10.35^{a,b,c}
Ellagic acid	–	42.36 ± 2.90^{f}	55.62 ± 4.86^{a,b}	17.23 ± 4.22^{b}	48.92 ± 8.32^{a,b,c,d}
Astragalin	–	36.56 ± 0.45^{e,f}	50.53 ± 4.78^{a,b}	20.45 ± 2.55^{b}	45.67 ± 9.89^{a,b,c,d}

Note: In each column, different superscripts represent significant differences ($p \leq 0.05$). ND; Not detectable.

longan leaf extract are the most potent anti-collagenase activity.

3.4. Anti-hyaluronidase activity

Hyaluronic acid is important in retaining the skin's moisture, structure, and elasticity. The degradation of hyaluronic acid contributes to diminishing dermal integrity. (Manuskiatti et al, 1996). As detailed in Table 1, all the fractions and the crude hydroethanolic extract possessed different anti-hyaluronidase activity at the reaction concentration of 250 µg/ml. However, fractions 1 and 2 were strongly anti-hyaluronidase with about 67.96 ± 8.16 and 63.82 ± 5.52% of inhibition, respectively, comparable to standards and more potent than hydroethanolic longan leaf extract.

3.5. Selection of the bioactive chemical marker (BCM) using AES

Chemical markers-based standardization plays a crucial role for manufacturers in the quality control of herbal products. The ideal markers are hopefully established and predicted for pharmacologic bioactivity, which can be applied in qualitative and quantitative assessment. (Ruiz et al., 2016). As the correlation between constituents and efficacy also plays a crucial role, influencing the constituent's role in botanical extract, the AES was applied to indicate the suitable BCM for hydroethanolic longan leaf extract (Yang et al., 2017). The activities of each fractionated extract, namely the inhibition ability, were defined as Efficacy Score (ES). The content of each fraction was employed in AES to represent the importance of the extract's efficacy. The ES and AES of each fraction are presented in Fig. 2. Fractions 1 and 2 present high overall ES values of about 249.02 and 235.96, respectively. However, the overall AES value of fraction 2 was not high because of the low yield in the extract. Fraction 7, the highest amount, presents the low overall AES value of 53.65%, while the maximum overall AES was fraction 1 with a value of 130.83%. Thus, fraction 1 was chosen for further selection and identification of BCM using LC-MS/MS analysis.

3.6. LC-MS/MS analysis of BCM

LC-MS/MS was performed for the identification of BCM in fraction 1. The gradient elution was performed instead of direct infusion mass spectrometry to check whether the samples were a mixture or pure substance. Fraction 1 was identified as a pure substance as the LC chromatogram presented a dominant peak at the retention of 12.243, as shown in Fig. 3(A). The molecular formula was assigned $C_9H_{10}O_5$ from MS spectra with the (M^-) ion peak at m/z 197.0467, shown in Fig. 3(B). The MS/MS spectra of fraction 1 were fragmented to form an ion at m/z 78.124, 124.0167(100%), 169.0149, presented in Fig. 3(C). The compound was fragmented to form a corresponding deprotonated ethyl gallate (Ousji and Sleno, 2022). Ethyl gallate (Fig. 4) is a gallate ester obtained by the formal condensation of gallic acid with ethanol which is a natural product found in many parts of longan, including seeds and leaves. It has been examined by multiple antioxidant systems, including DPPH radical scavenging capacity, deoxyri-

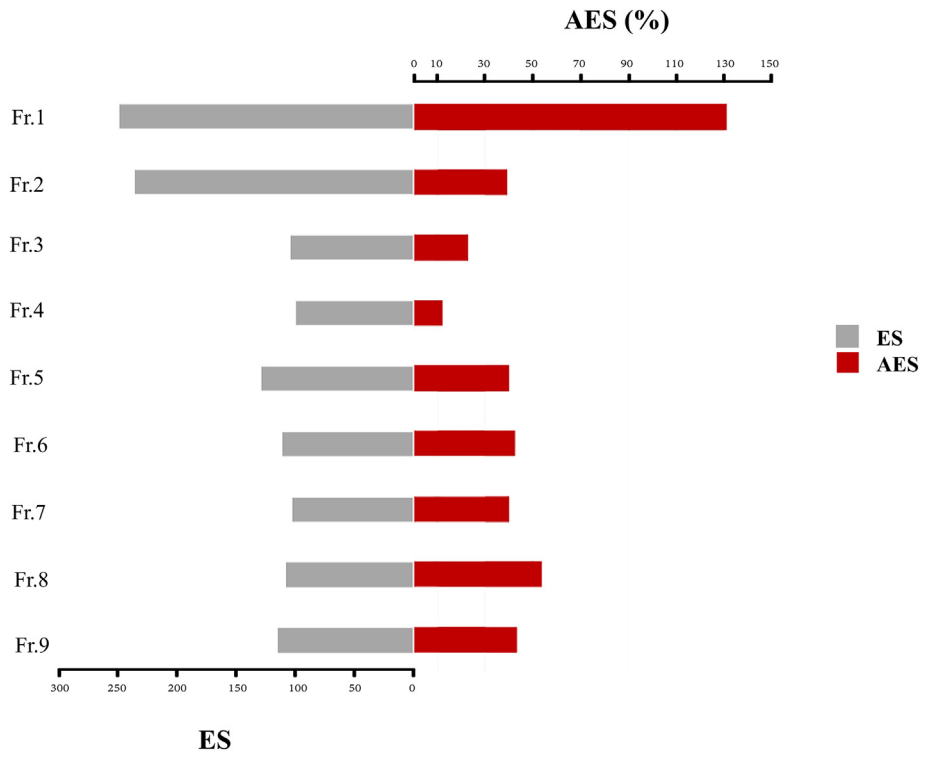

Fig. 2 Overall ES and AES values of each fractionated extract in hydroethanolic longan leaf extract.

bose degradation, β-carotene bleaching assay, hydrogen donor, a metal chelator and reduced potential as the potent antioxidant. (Kalaivani et al., 2011; Mai et al., 2020). Moreover, ethyl gallate was also reported to prevent lipid oxidation which proved more effective than gallic acid. The more hydrophobic gallate ester contributes greatly to bioavailability, presumably by increasing affinity for cell membranes and permeability (Zhao et al., 2021). Moreover, Ethyl gallate has also been reported to contain the abilities of collagenase and hyaluronidase inhibition (Barla et al., 2009). Furthermore, other fractions were also investigated. Fractions 2 to 5 were also identified as pure substances. Fraction 2 was identified as gallic acid with the (M^-) ion peak at m/z 169.0142, while fraction 5 was characterized as astragalin with the (M^-) ion peak at m/z 446.8000 (Chen et al., 2015; López-Fernández et al.,2020; Mai et al., 2020). Fractions 3 and 4 were unclear, with the (M^-) ion peak at m/z 354.9000 and 430.8000, respectively.

3.7. HPLC-UV analysis and correlations between bioactive compounds and biological activities

The fractionated extract and the hydroethanolic extract were analyzed by HPLC-UV analysis to confirm the correlation between bioactive compounds and biological activity. For this study, HPLC-UV analysis was performed for quantification. As shown in Fig. 5, ethyl gallate (fraction 1) could be identified with a retention time of 28.052. Gallic acid (fraction 2) was identified at a retention time of 6.428, while astragalin (fraction 5) was identified at 40.133. Ellagic acid was presented in fraction 6, while fractions 3, 7–9 could not be detected on the chromatogram. The area under chromatographic peaks of gallic acid, ethyl gallate, ellagic acid and astragalin was investigated after a month of storage under 4, 25, and 45 ± 0.5 °C. The storage was maintained until the amount of each compound significantly differed to find the relationship between the activities and the quantity of compounds. The correlations between the area under chromatographic peaks and biological activities after one month of storage of the extract solution are shown in Table 2.

Ethyl gallate showed a strong positive linear correlation ($p < 0.05$) among DPPH scavenging, lipid peroxidation inhibitory, anti-collagenase, and anti-hyaluronidase activity. ($r = 0.997$, 0.972, 0.998, and 0.998, respectively). Initial observation of the results suggests that ethyl gallate could be an attributable predictive ability between the compound level and these *in vitro* biological activities. Gallic and ellagic acid also showed a strong positive correlation to all activities; however, they were not statistically significant. These compounds may be involved in biological activity, or the activity may result from the compounds' combination. Contrary to phenolic compounds, the chromatographic area of astragalin and the others did not correlate to the biological activity. The current results were consistent with the related experiment in that the activity of the hydroethanolic longan leaf extract involved phenolic acids rather than flavonoids (Doungsaard et al., 2020).

Li et al. (2008) suggested eight categories of chemical markers: therapeutic, bioactive, characteristic, main, synergistic, correlative, toxic and general components. Therapeutic components dominate the direct therapeutic effects of a botanical extract. Bioactive components exhibit similar pharmacological effects as the whole extract. Synergistic components do not directly contribute to the therapeutic effects, but they act synergistically to enhance the bioactivity of other components. Characteristic components must be unique ingredients that may influence the therapeutic effects of a botanical extract. Main components are the most abundant in a botanical

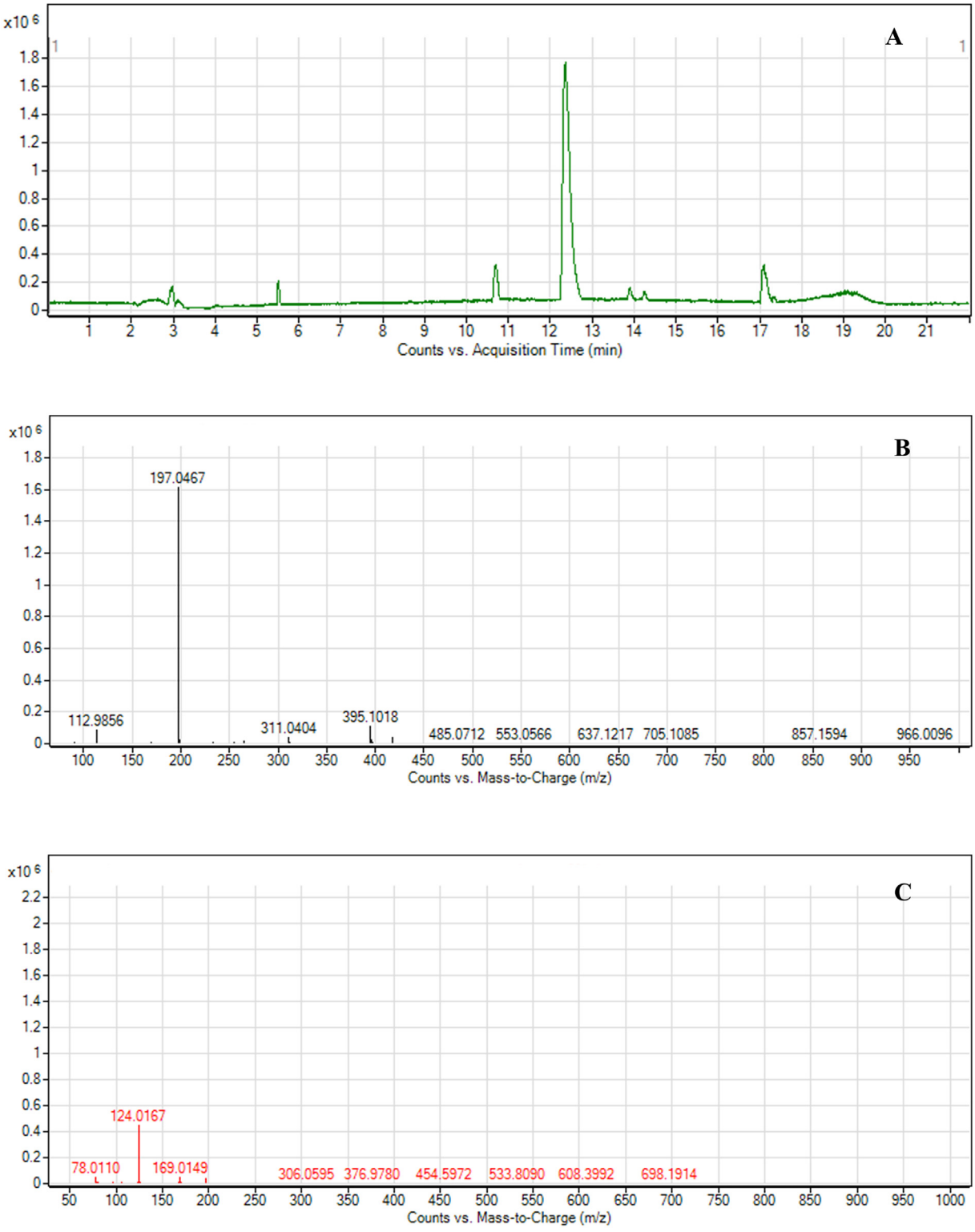

Fig. 3 LC-MS Chromatogram and MS spectra of fraction 1, (A) LC Chromatogram of fraction 1; (B) MS spectra of ethyl gallate; (C) MS-MS spectra of ethyl gallate.

extract. Correlative components, which may be a chemical or enzymatic reaction's precursors, products, or metabolites, are closely related. Toxic components are those presenting toxic therapeutics in botanical extract. The last marker is general components which are common and specific components present in a particular species, genus or family, which may be used as 'fingerprints' for quality control (Ruiz et al., 2016; Yang et al., 2017). The present study aims to select BCM for anti-aging assessment, which is established and predicted for the pharmacologic bioactivity of hydroethanolic longan leaf

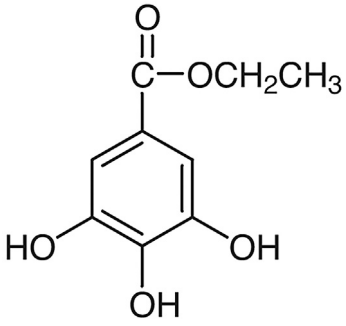

Fig. 4 Ethyl gallate structure.

extract for qualitative and quantitative application. Ethyl gallate was determined as the main component in the hydroethanolic longan leaf extract. Moreover, it could be selected as a bioactive component as it exhibits similar pharmacologic activities comparable to the whole extract. The correlations between the area under chromatographic peaks and biological activities after a month of storage of the extract solution showed a strong positive linear correlation. Thus, ethyl gallate could be used as a BCM for quality control of longan leaf extract. Gallic acid and ellagic acid were consid-

Table 3 The binding affinity of docked compounds found in hydroethanolic longan leaf extract with collagenase and hyaluronidase.

Compounds	Binding affinity (kcal/mol)	
	Collagenase (1CGL)	Hyaluronidase (2PE4)
Ethyl gallate	−6.8	−5.9
Gallic acid	−6.9	−6.0
Ellagic acid	−7.5	−7.8

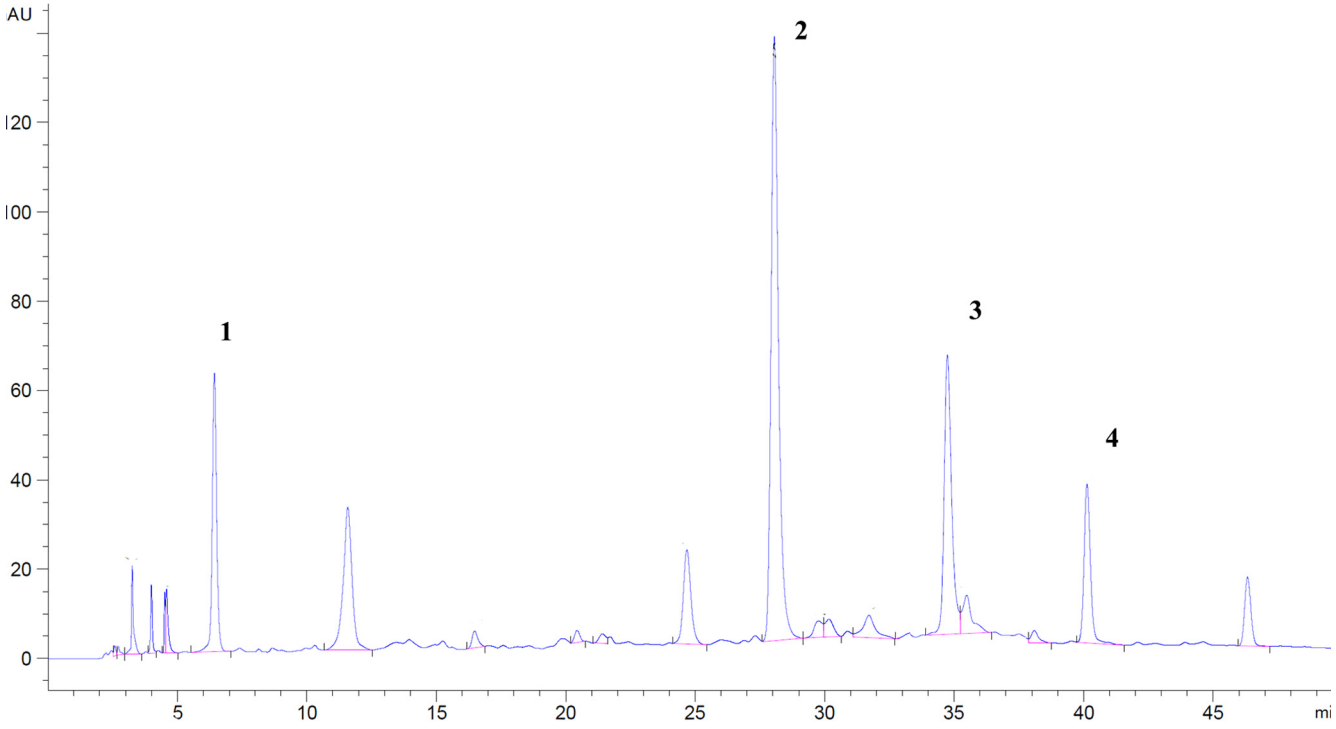

Fig. 5 HPLC chromatogram hydroethanolic *D.longan* leaf extract, (1) gallic acid, (2) ethyl gallate, (3) ellagic acid, and (4) astragalin.

Table 2 Pearson's correlation between the area under chromatographic peaks, total phenolic content and biological activities after one month of storage of extract solution.

Parameters	Pearson's correlation			
	DPPH assay	Lipid peroxidation inhibitory activity	Anti-collagenase actvity	Anti-hyaluronidase activity
Gallic acid	0.906	0.963	0.836	0.840
Ethyl gallate	0.997*	0.972*	0.998*	0.998*
Ellagic acid	0.762	0.618	0.847	0.844
Astragalin	−0.073	−0.269	0.071	0.065

*Significant at $p < 0.05$ (2-tailed).

ered for quality control's fingerprint as they possessed the same trend of biological activities as the extract. This knowledge provided essential information for pharmaceutical and cosmeceutical applications, including extraction, quality control and product development.

3.8. Molecular docking simulation

Molecular docking was performed to model the possible binding conformation of ethyl gallate, gallic acid and ellagic acid, which were selected for BCM and quality control's fingerprint, towards collagenase and hyaluronidase.

All compounds can form high interactions with collagenase and hyaluronidase. The binding affinity was retrieved and compared to each other, as shown in Table 3. Ellagic acid has the highest binding affinity towards collagenase and hyaluronidase, with docking scores of −7.5 and −7.8, respectively, followed by ethyl gallate and gallic acid.

Visualization analysis showed that all the potential compounds occupied the receptor's active site. Fig. 6(A) shows ethyl gallate and collagenase's structure and 3D protein–ligand interactions. Ethyl gallate formed four hydrogen bonds with Tyr237, Ser239, Arg214, and Glu219 amino acids and created hydrophobic interactions with Leu181. Fig. 6 (B) shows that gallic acid generated hydrogen bonds with Tyr237, Arg214, Leu181 and Ala182 of collagenase. Fig. 6 (C) shows interactions of ellagic acid, which has the highest affinity. Ellagic acid formed hydrogen bonds with Gly179, Glu219 and Tyr240 of collagenase. It also produced hydrophobic interaction with Leu181. The interactions of the hyaluronidase enzyme and each compound are shown in Fig. 7. Fig. 7 (A) shows the structure and 3D protein–ligand interactions of ethyl gallate

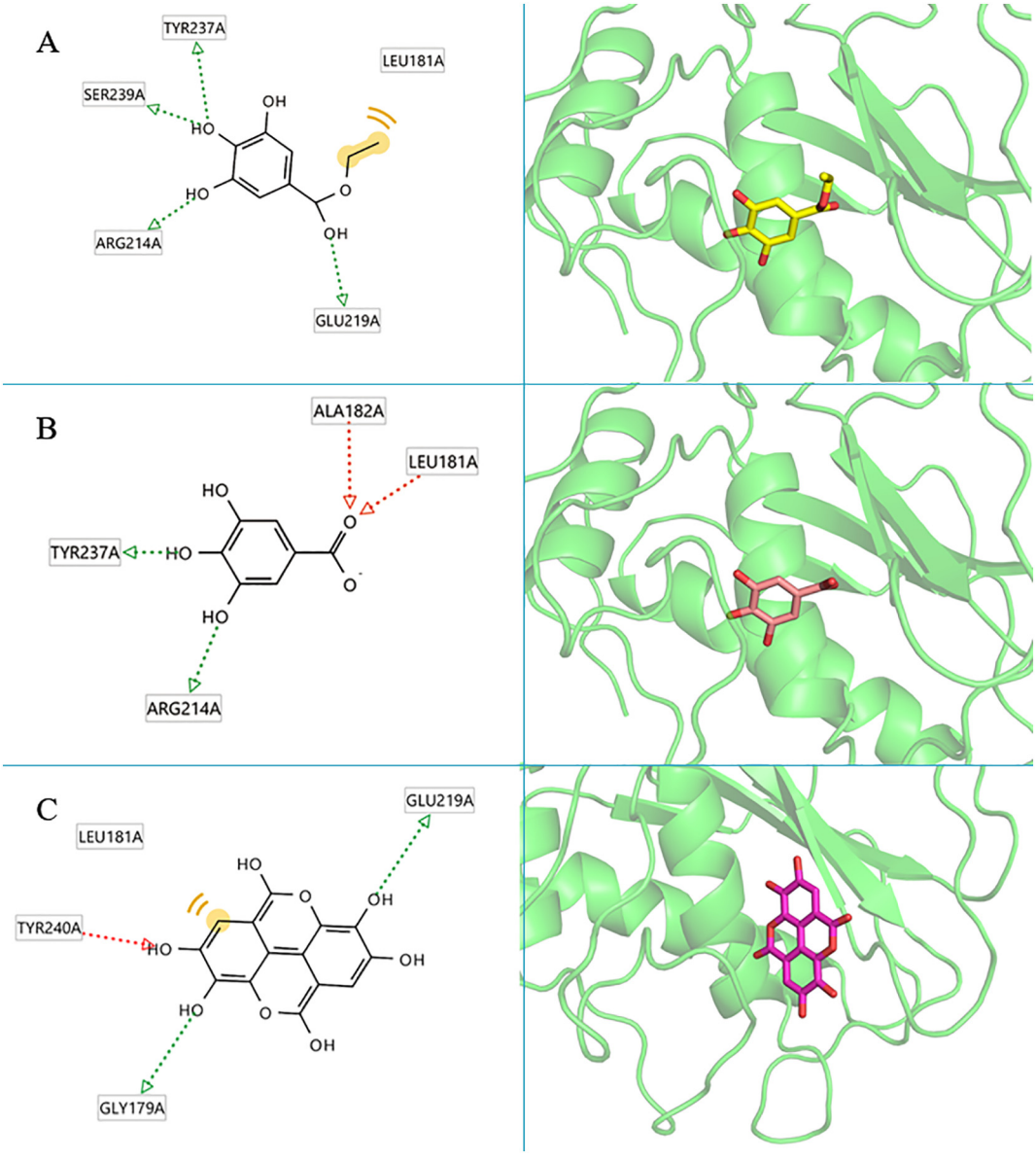

Fig. 6 The 2D and 3D protein–ligand interactions of each compound at the collagenase enzyme active site (PBD ID: 1CGL), (A) ethyl gallate, (B) gallic acid, (C) ellagic acid.

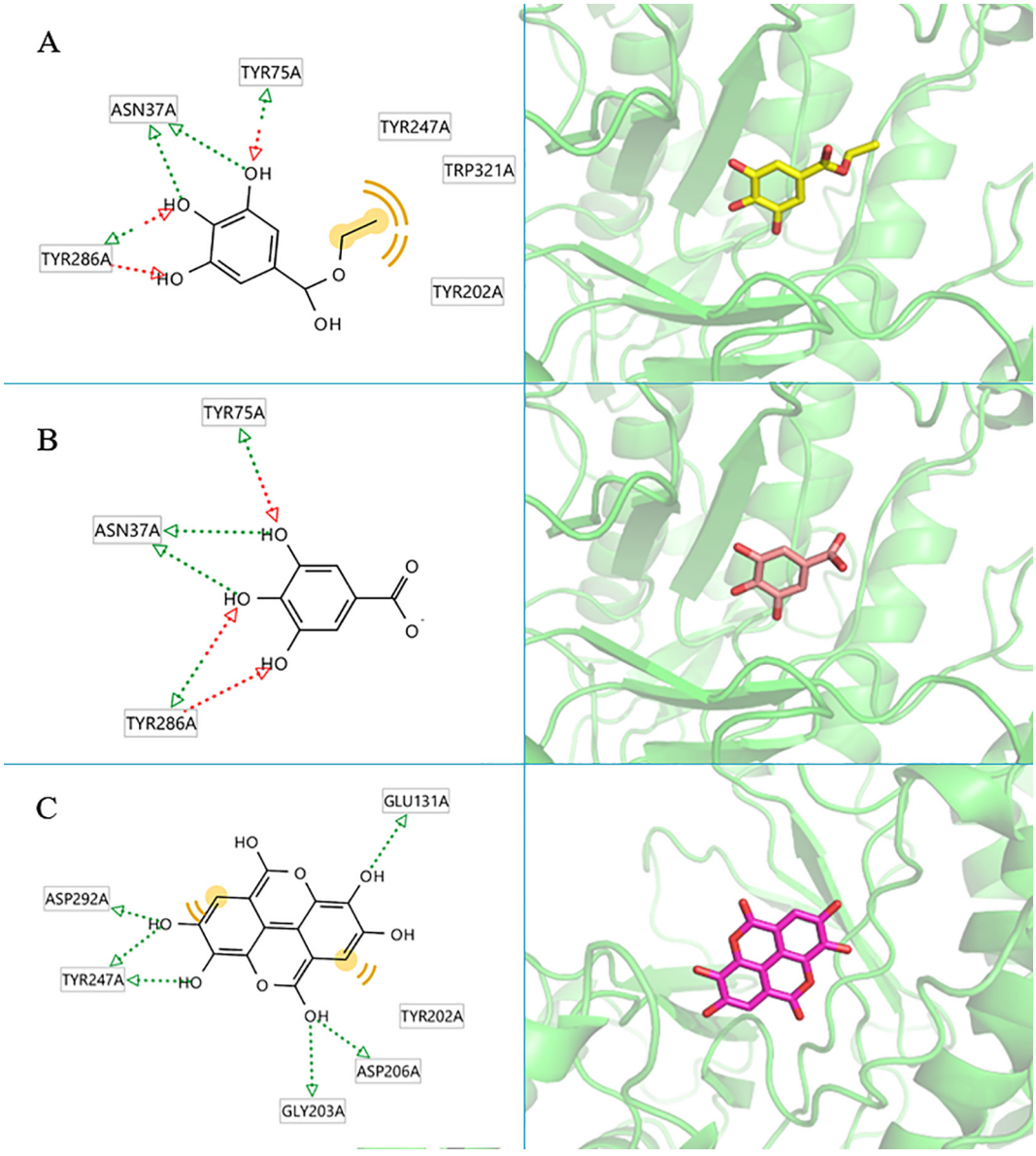

Fig. 7 The 2D and 3D protein–ligand interaction of each compound at the hyaluronidase enzyme active site (PBD ID: 2PE4), (A) ethyl gallate, (B) gallic acid, (C) ellagic acid.

with hyaluronidase. Ethyl gallate generated hydrogen bonds with Asn37, Tyr75 and Tyr286 and produced hydrophobic interaction with Tyr202, Tyr247, and Trp321. Similarly, Fig. 7 (B) shows that gallic acid generated hydrogen bonds with Tyr75, Asn37 and Tyr286. In addition, Fig. 7 (C) shows the interaction of ellagic acid, which has the highest affinity with hyaluronidase. Ellagic acid formed hydrogen bonds with Asp292, Tyr247, Gly203, Asp206 and Glu131 of hyaluronidase and produced hydrophobic interaction with Asp292 and Tyr202.

According to the molecular docking analysis of compounds found in hydroethanolic longan leaf extract with collagenase and hyaluronidase, it was inferred that ethyl gallate, ellagic acid and gallic acid could form interactions with good and acceptable binding affinity. The molecular docking analysis suggests a possible mechanism of action for these compounds.

4. Conclusion

In selecting a bioactive chemical marker via anti-aging assessment of hydroethanolic longan leaf extract, ethyl gallate possessed promising biological activities and a high proportion in the hydroethanolic longan leaf extract. The correlations between the area under chromatographic peaks on HPLC analysis of ethyl gallate and biological activities after one-month storage of the extract solution showed a strong positive linear correlation. The deterioration of ethyl gallate was a crucial factor in reducing anti-aging activity. The molecular docking of ethyl gallate to collagenase and hyaluronidase resulted in good, acceptable binding affinity. Therefore, it could be concluded that ethyl gallate is potentially used as a bioactive chemical marker for hydroethanolic longan leaf extract in pharmaceutical and cosmeceutical applications, including quality control and product development. Furthermore, gallic acid and ellagic acid were considered markers for chemical quality control.

Declaration of Competing Interest

The authors declare that they have no known competing financial interests or personal relationships that could have appeared to influence the work reported in this paper.

Acknowledgement

The authors would like to thank the Ph.D. Degree Program in Pharmacy, Faculty of Pharmacy, Chiang Mai University, Chiang Mai, Thailand 50200, under the CMU Presidential Scholarship, for providing financial support to conduct this study. Also, we would like to gratefully acknowledge the Faculty of Pharmacy, Chiang Mai University, Chiang Mai, Thailand 50200, for using all facilities.

References

Alam, M.N., Bristi, N.J., Rafiquzzaman, M., 2013. Review on *in vivo* and *in vitro* methods evaluation of antioxidant activity. Saudi. Pharm. J. 21 (2), 143–152. https://doi.org/10.1016/j.jsps.2012.05.002.

Barla, F., Higashijima, H., Funai, S., Sugimoto, K., Harada, N., Yamaji, R., Fujita, T., Nakano, Y., Inui, H., 2009. Inhibitive effects of alkyl gallates on hyaluronidase and collagenase. Biosci Biotechnol. Biochem. 73 (10), 2335–2337. https://doi.org/10.1271/bbb.90365.

Chao, K.L., Muthukumar, L., Herzberg, O., 2007. Structure of human hyaluronidase-1, a hyaluronan hydrolyzing enzyme involved in tumor growth and angiogenesis. Biochemistry 46 (23), 6911–6920.

Chen, Y., Yu, H., Wu, H., Pan, Y., Wang, K., Jin, Y., Zhang, C., 2015. Characterization and quantification by LC-MS/MS of the chemical components of the heating products of the flavonoids extract in pollen typhae for transformation rule exploration. Molecules. 20 (10), 18352–18366. https://doi.org/10.3390/molecules201018352.

Chen, G.L., Zhang, X., Chen, S.G., Han, M.D., Gao, Y.Q., 2017. Antioxidant activities and contents of free, esterified, and Insoluble-bound phenolics in 14 subtropical fruit leaves collected from the South of China. J. Funct. Foods. 30, 290–302. https://doi.org/10.1016/j.jff.2017.01.011.

Doungsaard, P., Chansakaow, S., Sirithunyalug, J., Shang-Chian, L., Wei-Chao, L., Chia-Hua, L., Ha, L., Leelapornpisid, P., 2020. *In vitro* biological activities of the anti-aging potential of *Dimocarpus longan* leaf extracts. CMU. J. Nat Sci. 19 (2), 235–251. https://doi.org/10.12982/CMUJNS.2020.0016.

Gerhäuser, C., 2009. Phenolic beer compounds to prevent cancer. In: Beer in health and disease prevention. Academic Press, pp. 669–684. https://doi.org/10.1016/B978-0-12-373891-2.00068-7.

Juan, C.A., Pérez de la Lastra, J.M., Plou, F.J., Pérez-Lebeña, E., 2021. The chemistry of reactive oxygen species (ROS) revisited: outlining their role in biological macromolecules (DNA, lipids and proteins) and induced pathologies. Int. J. Mol. Sci. 22 (9), 4642. https://doi.org/10.3390/ijms22094642.

Kalaivani, T., Rajasekaran, C., Mathew, L., 2011. Free radical scavenging, cytotoxic, and hemolytic activities of an active antioxidant compound ethyl gallate from leaves of *Acacia nilotica* (L.) Wild. Ex. Delile subsp. *Indica* (Benth.) Brenan. J. Food Sci. 76 (6), T144–T149. https://doi.org/10.1111/j.1750-3841.2011.02243.x.

Kamma, M., Lin, W.C., Lau, S-C., Chansakao w, S., Leelapornpisid, P., 2019. Anti-aging cosmeceutical product containing of *Nymphaea rubra* Roxb.ex *Andrews* extract. Chiang Mai J. Sci. 46(6), 1143-1160. Doi: 10.4103/0973-1296.182176.

Kolarsick, P.A., Kolarsick, M.A., Goodwin, C., 2011. Anatomy and physiology of the skin. J. Dermatol. Nurses' Assoc. 3 (4), 203–213. https://doi.org/10.1097/JDN.0b013e3182274a98.

Kurtz, A., Oh, S.J., 2012. Age related changes of the extracellular matrix and stem cell maintenance. Prev. Med. 54, S50–S56. https://doi.org/10.1016/j.ypmed.2012.01.003.

Li, S., Han, Q., Qiao, C., Song, J., Lung Cheng, C., Xu, H., 2008. Chemical markers for the quality control of herbal medicines: an overview. Chin. Med. 3 (1), 1–16. https://doi.org/10.1186/1749-8546-3-7.

Liu, Y., Liu, L., Mo, Y., Wei., C. LV., L., Luo, P., 2012. Antioxidant activity of longan (*Dimocarpus longan*) barks and leaves. Afr. J. Biotechnol. 11(27), 7038-7045. Doi: 10.5897/AJB11.3297.

López-Fernández, O., Domínguez, R., Pateiro, M., Munekata, P.E., Rocchetti, G., Lorenzo, J.M., 2020. Determination of polyphenols using liquid chromatography–tandem mass spectrometry technique (LC–MS/MS): A review. Antioxidants. 9 (6), 479. https://doi.org/10.3390/antiox9060479.

Lovejoy, B., Cleasby, A., Hassell, A.M., Longley, K., Luther, M.A., Weigl, D., Mcgeehan, G., Mcelroy, A.B., Drewry, D., Lambert, M. H., Jordan, S.R., 1994. Structure of the catalytic domain of fibroblast collagenase complexed with an inhibitor. Science. 263 (5145), 375–377. https://doi.org/10.1126/science.8278810.

Mai, J., Liang, J., Liu, X., Tan, L., Xu, H., Li, Y., Zhou, Y., Yang, C., Xin, C., 2020. Simultaneous determination of 5 components in the leaves of *Dimocarpus longan* by quantitative analysis of multi components by single marker (QAMS) based on UPLC and HPLC. J. Anal. Methods. Chem. https://doi.org/10.1155/2020/3950609.

Manuskiatti, W., Maibach, H.I., 1996. Hyaluronic acid and skin: wound healing and aging. Int. J. Dermatol. 35 (8), 539–544. https://doi.org/10.1111/j.1365-4362.1996.tb03650.x.

Medić-Šarić, M., Maleš, Ž., Stanić, G., Šarić, S., 1996. Evaluation and selection of optimal solvent and solvent combinations in thin-layer Chromatography of flavonoids and of phenolic acids of *Zizyphus jujuba* Mill. Croat. Chem. Acta. 69 (3), 1265–1274.

Morris, G.M., Huey, R., Lindstrom, W., Sanner, M.F., Belew, R.K., Goodsell, D.S., Olson, A.J., 2009. AutoDock4 and AutoDockTools4: Automated docking with selective receptor flexibility. J. Comput. Chem. 30 (16), 2785–2791. https://doi.org/10.1002/jcc.21256.

Naidoo, K., Birch-Machin, M.A., 2017. Oxidative stress and ageing: the influence of environmental pollution, sunlight, and diet on skin. Cosmetics. 4 (1), 4. https://doi.org/10.3390/cosmetics4010004.

Nichols, J.A., Katiyar, S.K., 2010. Skin photoprotection by natural polyphenols: anti-inflammatory, antioxidant, and DNA repair mechanisms. Arch. Dermatol. 302, 71–83. https://doi.org/10.1007/s00403-009-1001-3.

Ousji, O., Sleno, L., 2022. Structural elucidation of novel stable and reactive metabolites of green tea catechins and alkyl gallates by LC-MS/MS. Antioxidants. 11 (9), 1635. https://doi.org/10.3390/antiox11091635.

Paul, P., Biswas, P., Dey, D., Saikat, A.S.M., Islam, M., Sohel, M., Hossain, R., Mamun, A.A., Rahman, M.A., Hasan, M.N., Kim, B., 2021. Exhaustive plant profile of "*Dimocarpus longan* Lour" with significant phytomedicinal properties: a literature based-review. Processes. 9 (10), 1803. https://doi.org/10.3390/pr9101803.

Pittayapruek, P., Meephansan, J., Prapapan, O., Komine, M., Ohtsuki, M., 2016. Role of matrix metalloproteinases in photoaging and photocarcinogenesis. Int. J. Mol. Sci. 17 (6), 868. https://doi.org/10.3390/ijms1706086.

Rinnerthaler, M., Bischof, J., Streubel, M.K., Trost, A., Richter, K., 2015. Oxidative stress in aging human skin. Biomolecules. 5 (2), 545–589. https://doi.org/10.3390/biom5020545.

Ripa, F.A., Haque, M., Bulbul, I.J., 2010. *In vitro* antibacterial, cytotoxic and antioxidant of plant *Nephelium longan*. Pak. J. Biol. Sci. 13 (1), 22. https://doi.org/10.3923/pjbs.2010.22.27.

Ruiz, G.G., Nelson, E.O., Kozin, A.F., Turner, T.C., Waters, R.F., Langland, J.O., 2016. A lack of bioactive predictability for marker compounds commonly used for herbal medicine standardization. PloS one. 11 (7), e0159857.

Schrödinger, L., 2015. The PyMOL Molecular Graphics System. Version 1, 8.

Sharadha, M., Gowda, D.V., Gupta, V., Akhila, A.R., 2020. An overview on topical drug delivery system – Updated review. Int. J. Pharm. Sci. Res. Pharm. Sci. 11 (1), 368–385. https://doi.org/10.26452/ijrps.v11i1.1831.

Stewart, J.J.P., 2009. Application of the PM6 method to modeling proteins. J. Mol. Model. 15 (7), 765–805. https://doi.org/10.1007/s00894-008-0420-y.

Takahashi, T., Ikegami-Kawai, M., Okuda, R., Suzuki, K., 2003. A fluorimetric Morgan-Elson assay method for hyaluronidase activity. Anal. Biochem. 322 (2), 257–263. https://doi.org/10.1016/j.ab.2003. 08.005.

Trott, O., Olson, A.J., 2010. AutoDock Vina: improving the speed and accuracy of docking with a new scoring function, efficient optimization, and multithreading. J. Comput. Chem. 31 (2), 455–461. https://doi.org/10.1002/jcc.21334.

Wagner, H., Bladt, S., 1996. Plant Drug Analysis: A thin layer chromatography atlas. Springer Science & Business Media. https://doi.org/10.1007/978-3-642-00574-9.

Wolber, G., Langer, T., 2005. LigandScout: 3-D pharmacophores derived from protein-bound ligands and their use as virtual screening filters. J. Chem. Inf. Model. 45 (1), 160–169.

Xue, Y., Wang, W., Liu, Y., Zhan, R., Chen, Y., 2015. Two new flavonol glycosides from *Dimocarpus longan* leaves. Nat. Prod. Res. 29 (2), 163–168. https://doi.org/10.1080/14786419.2014.971318.

Yang, Z., Shao, Q., Ge, Z., Ai, N., Zhao, X., Fan, X., 2017. A bioactive chemical markers based strategy for quality assessment of botanical drugs: Xuesaitong injection as a case study. Sci. Rep. 7 (1), 2410. https://doi.org/10.1038/s41598-017-02305-y.

Yasmin, H., Kabashima, T., Rahman, M.S., Shibata, T., Kai, M., 2014. Amplified and selective assay of collagens by enzymatic and fluorescent reactions. Sci. Rep. 4 (1), 1–8. https://doi.org/10.1038/srep04950.

Zhao, M.T., Liu, Z.Y., Li, A., Zhao, G.H., Xie, H.K., Zhou, D.Y., Wang, T., 2021. Gallic acid and its alkyl esters emerge as effective antioxidants against lipid oxidation during hot air drying process of *Ostrea talienwhanensis*. LWT-Food Sci. Technol. 139, 11051. https://doi.org/10.1016/j.lwt.2020.110551.